

Absence of Luther-Emery Phase in the Three-Band Model for Cuprate Ladders

Jeong-Pil Song,¹ Sumit Mazumdar,¹ R. Torsten Clay^{2*}

¹Department of Physics, University of Arizona Tucson, AZ 85721,

²Department of Physics & Astronomy, and HPC² Center for Computational Sciences,
Mississippi State University, Mississippi State, MS 39762

*To whom correspondence should be addressed; E-mail: r.t.clay@msstate.edu.

Correlated-electron theories of superconductivity in cuprates often start from the premise of a gapped spin-liquid phase proximate to the superconducting state. This assumption is based on, (i) demonstrations of a Luther-Emery phase with dominant superconducting correlations in the doped 2-leg one-band Hubbard ladder, and (ii) the perceived analogy between coupled ladders and the square lattice. We demonstrate from accurate density matrix renormalization group calculations the absence of the Luther-Emery phase in the doped 2-leg three-band ladder consisting of both copper and oxygen. For realistic oxygen-oxygen hopping and Hubbard repulsion on the oxygen atoms, the decay of the superconducting pair correlation with distance is almost indistinguishable from that of free fermions. Our results cast severe doubts on many of the existing correlated-electron theories of superconductivity.

More than three decades after the discovery of high temperature superconductivity (SC) in cuprates, there is no consensus on the mechanism of the phenomenon. There is broad agreement that the undoped parent semiconducting antiferromagnetic compounds can be described within

the Cu-only one-band two-dimensional (2D) Hubbard model, which ignores the O-ions entirely. Proximity of SC to antiferromagnetism has led to the widely held belief that the mechanism of SC can also be found within an effective weakly-doped single-band Hubbard model (1–3), based on the claim that the spins on the Cu-sites and on the dopant-induced holes on the O-sites form local spin-singlets that behave like double occupancies in the single-band Hubbard model (4). The list of approximate correlated-electron theories that find SC within the weakly doped one-band Hubbard model is long, but accurate numerical studies have consistently found that superconducting correlations are suppressed by the Hubbard U for carrier concentrations believed to be appropriate for the superconductors (5, 6). Recent very careful study using two distinct and complementary numerical approaches to calculating superconducting pair-pair correlations has concluded that SC is absent in the square lattice within the model (7). Inclusion of second neighbor hopping t' beyond the nearest neighbor (n.n.) (8) does not change this conclusion, irrespective of the relative sign of this quantity (9, 10), even as there are signatures of enhanced pair correlations at $\frac{1}{4}$ -filling (11), far from the carrier concentration believed to be appropriate for the cuprates.

A key reason for the continued application of the one-band Hubbard model to cuprates is the repeated finding that the ground state of the weakly doped 2-leg one-band Hubbard ladder is a Luther-Emery liquid, with gapless charge and gapped spin modes (12, 13). Such a spin-gap proximity effect has been considered essential for SC within an entire class of theories (1, 2, 14). DMRG calculations, known to be highly precise for one dimensional (1D) Hamiltonians, find slower than $1/r$ decay of the superconducting pair-pair correlation $P(r)$ in the doped 2-leg one-band Hubbard ladder, where r is the interpair separation (15–17). Strong superconducting correlations in the doped ladder is a consequence of spin-singlet formation on the undoped ladder rungs (18). The DMRG results therefore have lent credence to the viewpoint that some variant of the 2D one-band Hubbard model with minor modifications might still yield SC. Some

authors have suggested that the 2D lattice can be considered as coupled ladders (19, 20).

A realistic description of the cuprate ladder, however, should include the O-ions (see Fig. 1). Surprisingly, few authors have investigated the appropriateness of replacing the more complete three-band 2-leg ladder Hamiltonian that includes the O-ions with the one-band Hubbard Hamiltonian (21, 22). We have performed accurate DMRG calculations on long three-band 2-leg ladders for parameters appropriate for real cuprates. We find that superconducting pair correlations are strongly suppressed within the three-band model, a result with profound implications.

The one-band ladder Hamiltonian has parameters U , the Hubbard repulsion; and the leg and rung hopping integrals t and t_{\perp} , respectively. It is customary to express U and $|t_{\perp}|$ in units of $|t|$. We consider the three-band ladder Hamiltonian,

$$\begin{aligned}
H = & \Delta_{\text{dp}} \sum_{i\sigma} p_{i,\sigma}^{\dagger} p_{i,\sigma} - \sum_{\langle ij \rangle, \lambda, \sigma} t_{\text{dp}}^{\perp} (d_{i,\lambda,\sigma}^{\dagger} p_{j,\sigma} + H.c.) \\
& - \sum_{\langle ij \rangle, \lambda, \sigma} t_{\text{dp}} (d_{i,\lambda,\sigma}^{\dagger} p_{j,\sigma} + H.c.) - \sum_{\langle ij \rangle, \sigma} t_{\text{pp}} (p_{i,\sigma}^{\dagger} p_{j,\sigma} + H.c.) \\
& + U_{\text{d}} \sum_{i,\lambda} d_{i,\lambda,\uparrow}^{\dagger} d_{i,\lambda,\uparrow} d_{i,\lambda,\downarrow}^{\dagger} d_{i,\lambda,\downarrow} + U_{\text{p}} \sum_j p_{j,\uparrow}^{\dagger} p_{j,\uparrow} p_{j,\downarrow}^{\dagger} p_{j,\downarrow}
\end{aligned} \tag{1}$$

Here $d_{i,\lambda,\sigma}^{\dagger}$ creates a hole with spin σ on the i th Cu $d_{x^2-y^2}$ orbital on the λ -th leg ($\lambda = 1, 2$), $p_{j,\sigma}^{\dagger}$ creates a hole on the n.n. rung oxygen O_{R} or leg oxygen O_{L} ; t_{dp}^{\perp} and t_{dp} are n.n. ladder rung and leg Cu-O hopping integrals and t_{pp} is the n.n. O-O hopping integral. U_{d} and U_{p} are the onsite repulsions on the Cu and O sites, and $\Delta_{\text{dp}} = \epsilon_p - \epsilon_d$ where ϵ_p (ϵ_d) is the site energy of O (Cu). In what follows all energies are in units of $|t_{\text{dp}}|$. Most of our calculations are for $t_{\text{dp}} = t_{\text{dp}}^{\perp} = 1$, $U_{\text{d}} = 8$, $\Delta_{\text{dp}} = 3$; we show a few results also for $t_{\text{dp}}^{\perp} > 1$. We show results for two different $t_{\text{pp}} = 0, 0.5$ and also two different $U_{\text{p}} = 0, 3$. These parameters (with $t_{\text{pp}} = 0.5$ and $U_{\text{p}} = 3$) are nearly identical to those used previously (21, 22). They are also very close to those derived from recent first principles calculations (23). Our calculations are performed for different dopings δ , where $1 - \delta$ is the average hole concentration per Cu-ion ($\delta = 0$ for the undoped ladder).

In Table 1 we have given the calculated $L \rightarrow \infty$ extrapolated charges (see Supplementary Materials (SM) for the details of the extrapolation procedure) on the Cu-ions $\langle n_{Cu} \rangle$, rung O-ions $\langle n_{O_R} \rangle$ and leg O-ions $\langle n_{O_L} \rangle$, respectively, for $\delta = 0$ and $\delta = 0.125$, which are representative for other δ (see SM). The doping-induced increase in $\langle n_{Cu} \rangle$ is very small, with the bulk of the doped charge going to O-ions. Importantly, given that there occur two leg O-ions corresponding to each rung O, the overall increase in population due to doping is larger for O_L than O_R . Our calculated charge-densities are close to those obtained previously for shorter three-band ladders for similar parameters (22).

Fig. 2(a) shows the extrapolated spin gaps $\Delta_S = E(S_z = 1) - E(S_z = 0)$, where $E(\dots)$ is the lowest energy of the state with total z -component of spin S_z , for $\delta = 0$, $t_{dp}^\perp = 1$ and for a range of U_d for $U_p = U_d/2$ (see SM for details of the extrapolation procedure). For parameters for which previous calculations exist in the literature (for e.g., $U_d = 8$, $t_{dp}^\perp = 1$, $t_{pp} = U_p = 0$) our calculated Δ_S are the same as before (21). The increase in Δ_S with t_{pp} for $\delta = 0$ has been noted before (22), and can be understood within perturbation theory. Nonzero U_p suppresses Δ_S strongly. The behavior of Δ_S versus $U_d/|t_{pd}|$ is very similar to that versus $U/|t|$ in one-band ladders, where also a maximum near $U/|t| = 8$ is observed (15). Undoped three- and one-band models are thus indeed similar.

In Fig. 2(b) we have shown the doping dependence of the extrapolated spin gaps (See SM for details of the extrapolations). We have included additional data points for $t_{dp}^\perp = 1.25$ here. Δ_S is suppressed strongly with doping, as is also true within the one-band ladder. What is new, however, is the strong enhancement of Δ_S in the undoped state when $t_{pp} \neq 0$, as noted above, but very rapid suppression of the same upon doping. The very large Δ_S for $\delta = 0$, $t_{dp}^\perp = 1.25$, along with $\Delta_S \simeq 0$ for the doped case here are in agreement with previous one-band calculation of the spin gap in the doped ladder for $U = 8$ and $t_\perp/t > 1.5$. The very rapid diminishing of Δ_S with doping already suggests the suppression of the superconducting correlations we find

(see below).

We define $P_i^\dagger = (d_{i,1,\uparrow}^\dagger d_{i,2,\downarrow}^\dagger - d_{i,1,\downarrow}^\dagger d_{i,2,\uparrow}^\dagger)$ and calculate the pair-pair correlation function $P(r) = \langle P_i^\dagger P_j \rangle$, with $r = |i - j|$. Fig. 3 shows the ladder length dependence of $P(r)$ for two different parameters sets, Fig. 3(a) with $U_p = t_{pp} = 0$ and Fig. 3(b) with $U_p = 3$ and $t_{pp}=0.5$. For all of the ladder lengths and parameter values we studied, $P(r)$ was well fit by a power law $r^{-\alpha}$ provided short and long distances are excluded. These limits are due to finite size effects and are well understood in the case of the one-band ladder (17). In particular, we verified that the sharp decrease in $P(r)$ at the largest r in Figs. 3 and 4 is a finite-size effect and not due insufficiently large DMRG m . As seen in Fig. 3(a), for $U_p = t_{pp} = 0$ we find $\alpha \sim 1$. With more realistic parameters, $U_p = 3$ and $t_{pp} = 0.5$, we find the power law exponent α close to 2. (see Fig. 3(b)). In Fig. 4 we show power-law fits for $\delta = 0.0625$ (Fig. 4(a)) and $\delta = 0.1250$ (Fig. 4(b)) for the 64-rung ladder. Nonzero U_p and t_{pp} both suppress $P(r)$, and when *both* are nonzero the suppression of $P(r)$ is further increased. As in the one-band ladder, we find that α increases rapidly with doping (17). For $U_p = 3$, $t_{pp} = 0.5$, and $\delta = 0.1250$, the decay of $P(r)$ with distance is indistinguishable from that of noninteracting fermions, for which $\alpha = 2$.

The suppression of the pair-pair correlations within the three-band model is consistent with similar observation of the same for large rung hopping $t_\perp > t$ within the one-band model (see Fig. 6 in reference (16)). As seen in reference (16) not only is the pair-pair correlation suppressed by large t_\perp , the suppression occurs at smaller and smaller t_\perp (that are however > 1) as the Hubbard repulsion U increases. Within the same range of U the spin gap in the undoped one-band ladder *increases* with U . It therefore follows that increase in the spin gap in the undoped one-band ladder is accompanied by concomitant increase of pair correlations in the doped ladder, only until a maximum in the undoped ladder spin gap is reached. Beyond this maximum, further increase of the spin gap in the undoped single-band ladder results in suppression of the pair-pair correlations in the doped ladder. *Our results in Figs. 4 indicate that*

this maximum in the spin gap of the undoped three-band ladder has been reached already at $t_{\text{dp}}^{\perp} = 1$.

The physical explanation of the rapid suppression of the pair-pair correlation is as follows. Superconducting pairing in both one- and three-band ladder Hamiltonians can be understood within an *effective* Hamiltonian of the form,

$$H_{\text{eff}} = \sum_i J(\delta) P_i^{\dagger} P_i - t_{\text{pair}} \sum_{\langle i,j \rangle} P_i^{\dagger} P_j - t_f \sum_{\langle \mu,\nu \rangle, \sigma} f_{\mu,\sigma}^{\dagger} f_{\nu,\sigma} \quad (2)$$

where $J(\delta)$ is proportional to the self-consistent spin gap at doping δ , t_{pair} the effective pair hopping integral, and t_f refers to single-particle fermion hops. As in Eq. (1), i, j refer to rung indices. While μ, ν also refer to nearest neighbor rungs in the one-band ladder, they refer to both Cu- and O-sites in the three-band ladder. Within the one-band model, t_{pair} and t_f are related, with $t_{\text{pair}} \sim t_f^2 / \Delta_{\text{pb}}$, where Δ_{pb} is the pair-binding energy, roughly proportional to the spin gap in the undoped ladder.

The interactions $J(\delta)$ and t_{pair} , taken together, dominate over the pair-breaking single-particle t_f over a broad range of parameters in the one-band ladder, including in particular $t_{\perp} = 1$. This situation is altered significantly within the three-band model. The doped holes now enter primarily O-sites (see Table 1), and the complete spin-singlet wavefunction involves not only the Cu-ions but also the rung O-ion and the four ladder oxygens on either side of the rung. Pair motion now must involve not only the the doped charges on the Cu-ions of a rung, but also those on the neighboring O-ions, making the effective mass of the spin-singlet within the three-band model significantly larger than in the one-band model. At the same time, however, t_f now can involve the holes on the O-ions exclusively, with the Cu-ion holes playing a very limited role (*i.e.*, t_f now includes and is even dominated by t_{pp}). Single-particle hopping thus has a far stronger pair-breaking effect in the three-band ladder. It now becomes obvious why the strongest suppression of the doped-state spin gap and superconducting pair correlations occur

within the Hamiltonians with nonzero t_{pp} (see Figs. 2(b) and 4).

Our theoretical results demonstrate that, (i) conclusions regarding pairing based on effective single-band ladder models cannot be extended to the three-band ladder, and (ii) there is no pairing within the three-band ladder for realistic cuprate parameters (we emphasize that the value of U_p we have chosen is a lower limit (23), and U_p uniformly suppresses pairing.) The absence of SC in the 2-leg ladder compound $\text{La}_{2-x}\text{Sr}_x\text{CuO}_{2.5}$ (24) is expected within our theory. Superconducting $\text{Sr}_{14-x}\text{Ca}_x\text{Cu}_{24}\text{O}_{41}$ consists of alternating planes of corner-sharing CuO_2 chains and edge-sharing Cu_2O_3 ladders (25–27). It is believed that there occur nearly 5 holes per formula unit (f. u.) on chains and 1 hole per f. u. on ladders at $x = 0$. There occurs some transfer of holes from chain to ladder with increasing x , but the actual extent of the transfer is not agreed upon. The appearance of SC above 4.0 GPa in $x = 11.5$ single crystals is accompanied by a 1D-to-2D dimensional crossover, as evidenced from the insulator-like resistivity ρ_a along the rung-axis a at all temperatures below the critical pressure and metallic ρ_a at all temperatures above this pressure (26). The resistivity ratio ρ_a/ρ_c (the c -axis corresponds to the ladder leg direction) of the $x = 11.5$ compound decreases by one to two orders of magnitude at low temperature and high pressure (26). There occurs a concomitant decrease in the a -axis lattice parameter, although at still higher pressure where superconducting T_c decreases the lattice parameter increases again. ^{63}Cu and ^{17}O NMR studies for the $x = 12$ compound have found that the spin gap decreases sharply with pressure, and there appear low-lying spin excitations, indicating the presence of mobile quasi-particles that contribute to a finite density of states at the Fermi level and perhaps also SC (28, 29). Taken together, these observations, (i) indicate clearly that the origin of SC in $\text{Sr}_{14-x}\text{Ca}_x\text{Cu}_{24}\text{O}_{41}$ cannot be found within ladder-based theories (27), and (ii) are consistent with our finding that superconducting correlations are absent in the three-band ladder Hamiltonian with realistic U_p and t_{pp} .

Our results raise a fundamental (and disturbing) question. What is the implication of the ab-

sence of a Luther-Emery phase (12) in the three-band 2-leg ladder Hubbard Hamiltonian for the 2D CuO₂ layer? As mentioned above, the existence of a gapped spin-liquid phase proximate to the superconducting state is assumed within a very large fraction of the theories of correlated-electron superconductivity in cuprates. As with the 2D one-band Hubbard Hamiltonian direct numerical computation of $d_{x^2-y^2}$ pair correlations within the three-band Hamiltonian for the CuO₂ layer also found absence of SC (30). As of now there is no clear understanding of the transition to the pseudogap state in the hole-doped cuprates or the pressure-induced dimensionality crossover in Sr_{14-x}Ca_xCu₂₄O₄₁ (26). At the same time, charge-ordered states have been found in the layered hole- and electron-doped cuprates as well as in Sr_{14-x}Ca_xCu₂₄O₄₁. Taken together, these results point to a web of contradictions which needs to be untangled in order to reach a comprehensive theory of SC in the cuprates (31).

References

1. P. W. Anderson, G. Baskaran, Z. Zou, T. Hsu, *Phys. Rev. Lett.* **58**, 2790 (1987).
2. P. A. Lee, N. Nagaosa, X. G. Wen, *Rev. Mod. Phys.* **78**, 17 (2006).
3. D. J. Scalapino, *Rev. Mod. Phys.* **84**, 1383 (2012).
4. F. C. Zhang, T. M. Rice, *Phys. Rev. B* **37**, 3759(R) (1988).
5. S. Zhang, J. Carlson, J. E. Gubernatis, *Phys. Rev. Lett.* **78**, 4486 (1997).
6. T. Aimi, M. Imada, *J. Phys. Soc. Jpn.* **76**, 113708 (2007).
7. M. Qin, *et al.*, *Phys. Rev. X* **10**, 031016 (2020).
8. H. C. Jiang, T. P. Devereaux, *Science* **365**, 1424 (2019).
9. Z. B. Huang, H. Q. Lin, J. E. Gubernatis, *Phys. Rev. B* **64**, 205101 (2001).

10. C.-M. Chung, M. Qin, S. Zhang, U. Schollwöck, S. R. White, *Phys. Rev. B* **102**, 041106 (2020).
11. N. Gomes, W. W. De Silva, T. Dutta, R. T. Clay, S. Mazumdar, *Phys. Rev. B* **93**, 165110 (2016).
12. A. Luther, V. J. Emery, *Phys. Rev. Lett.* **33**, 589 (1974).
13. L. Balents, M. P. A. Fisher, *Phys. Rev. B* **53**, 12133 (1996).
14. V. J. Emery, S. A. Kivelson, O. Zachar, *Phys. Rev. B* **56**, 6120 (1997).
15. R. M. Noack, S. R. White, D. J. Scalapino, *Phys. Rev. Lett.* **73**, 882 (1994).
16. R. M. Noack, N. Bulut, D. J. Scalapino, M. G. Zacher, *Phys. Rev. B* **56**, 7162 (1997).
17. M. Dolfi, B. Bauer, S. Keller, M. Troyer, *Phys. Rev. B* **92**, 195139 (2015).
18. E. Dagotto, T. M. Rice, *Science* **271**, 618 (1996).
19. E. Arrigoni, E. Fradkin, S. A. Kivelson, *Phys. Rev. B* **69**, 214519 (2004).
20. K. L. Hur, T. M. Rice, *Ann. Phys.* **324**, 1452 (2009).
21. E. Jeckelmann, D. J. Scalapino, S. R. White, *Phys. Rev. B* **58**, 9492 (1998).
22. S. Nishimoto, E. Jeckelmann, D. J. Scalapino, *Phys. Rev. B* **66**, 245109 (2002).
23. M. Hirayama, Y. Yamaji, T. Misawa, M. Imada, *Phys. Rev. B* **98**, 134501 (2018).
24. Z. Hiroi, M. Takano, *Nature* **377**, 41 (1995).
25. M. Uehara, *et al.*, *J. Phys. Soc. Jpn.* **65**, 2764 (1996).
26. T. Nagata, *et al.*, *Phys. Rev. Lett.* **81**, 1090 (1998).

27. T. Vuletić, *et al.*, *Phys. Rep.* **428**, 169 (2006).
28. Y. Piskunov, D. Jérôme, P. Auban-Senzier, P. Wzietek, A. Yakubovsky, *Phys. Rev. B* **69**, 014510 (2004).
29. N. Fujiwara, *et al.*, *Phys. Rev. B* **80**, 100503(R) (2009).
30. M. Guerrero, J. E. Gubernatis, S. Zhang, *Phys. Rev. B* **57**, 11980 (1998).
31. S. Mazumdar, *Phys. Rev. B* **98**, 205153 (2018).
32. M. Fishman, S. R. White, E. M. Stoudenmire (2020). <https://arxiv.org/abs/2007.14822>.
33. J. Towns, *et al.*, *Computing in Science & Engineering* **16**, 62 (2014).
34. N. A. Nystrom, M. J. Levine, R. Z. Roskies, J. R. Scott, *Proceedings of the 2015 XSEDE Conference: Scientific Advancements Enabled by Enhanced Cyberinfrastructure*, XSEDE '15 (ACM, New York, NY, USA, 2015), pp. 30:1–30:8.

Methods

Our DMRG calculations are done with open boundary conditions, with Cu-O-Cu rungs at both ends (see Fig. 1). Calculations used the ITensor library (32) with a two-site DMRG update and particle number and S_z conservation. We have considered ladders with length L up to 40 rungs (198 sites) for the undoped case, and with up to $L = 64$ (318 sites) for doped cases, with bond dimension m up to 12,000. The minimum DMRG truncation error was of order 10^{-8} ; we extrapolated energies and correlation functions to zero truncation error as detailed in the SM. These are the longest three-band ladder calculations with the largest m to date.

Because of the open boundary conditions, for each value of $P(r)$ we average N_{avg} values of $\langle P_i^\dagger P_j \rangle$ with the rungs i and j symmetrically placed about the center of the ladder, with

N_{avg} taken to be 11 (12) for odd (even) r (17). The choice of N_{avg} does not influence the distance dependence of $P(r)$. The error bars on $P(r)$ in Figs. 3 and 4 are based on the standard deviation of $P(r)$ in this averaging process, which we find to be larger than the error of the DMRG truncation extrapolation.

Acknowledgments

Work at Arizona was supported by NSF-CHE-1764152. Some calculations in this work used the Extreme Science and Engineering Discovery Environment (33) (XSEDE), which is supported by National Science Foundation grant number ACI-1548562. Specifically, we used the Bridges system (34) which is supported by NSF award number ACI-1445606, at the Pittsburgh Supercomputing Center under award TG-DMR190068.

Author Contributions

JPS and RTC performed the DMRG calculations. RTC developed the DMRG codes. SM wrote the manuscript.

Competing Interests

The authors declare no competing interests.

Supplementary materials

Supplementary Text

Figs. S1 to S8

Figures and Tables

Table 1: Average extrapolated charge densities on Cu and O-sites in the undoped and doped ($\delta = 0.125$) three-band Hubbard Hamiltonian for $U_d = 8$.

U_p	t_{pp}	$\langle n_{Cu} \rangle$		$\langle n_{O_R} \rangle$		$\langle n_{O_L} \rangle$	
		$\delta=0$	$\delta=0.125$	$\delta=0$	$\delta=0.125$	$\delta=0$	$\delta=0.125$
0	0.0	0.81	0.82	0.13	0.19	0.12	0.20
0	0.5	0.73	0.75	0.22	0.28	0.15	0.22
3	0.0	0.82	0.84	0.12	0.18	0.12	0.19
3	0.5	0.75	0.78	0.20	0.26	0.14	0.21

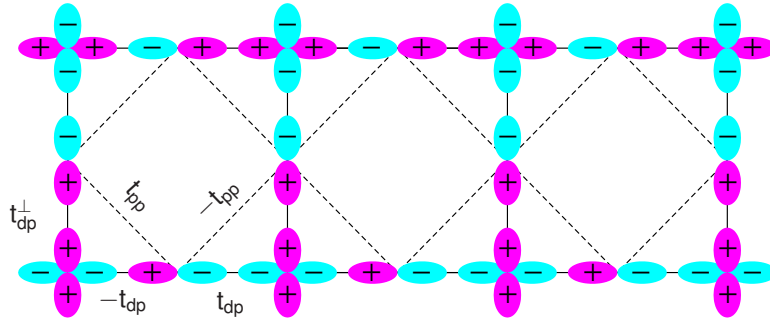


Figure 1: (Color online) Lattice structure of the three-band 2-leg ladder we investigate.

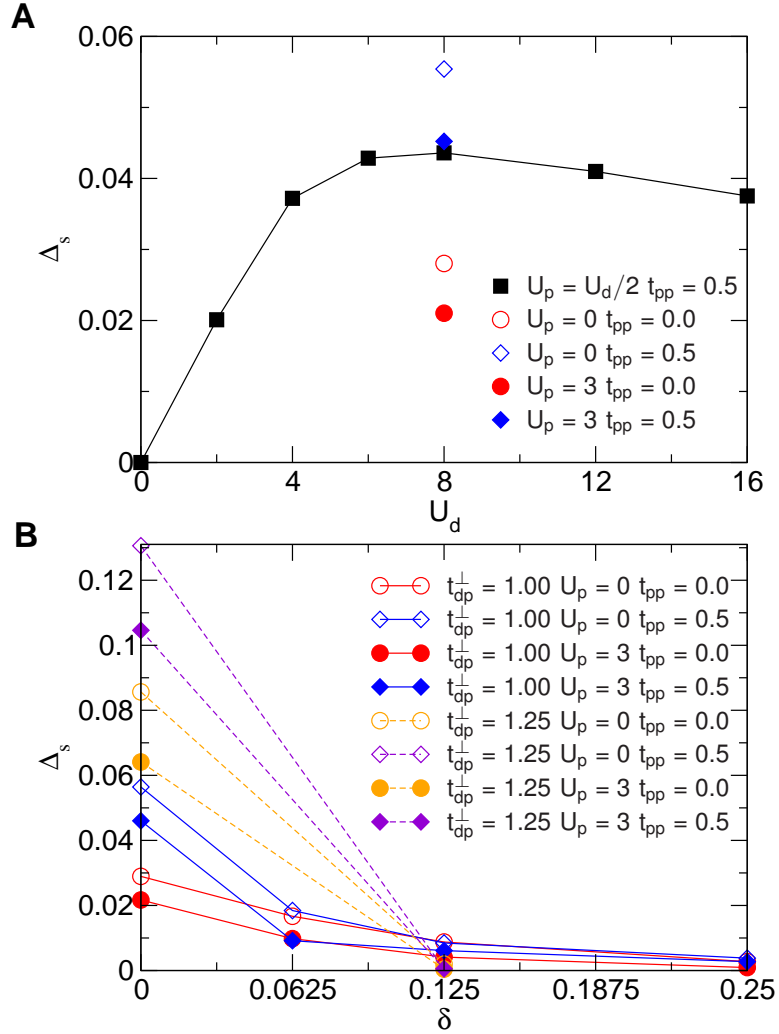


Figure 2: (Color online) (a) Spin gap versus U_d in the undoped three-band ladder. In all cases $t_{dp}^\perp = 1$. (b) Same as a function of doping δ . Solid (dotted) lines correspond to $t_{dp}^\perp = 1$ ($t_{dp}^\perp = 1.25$). Lines are guides to the eye. DMRG truncation and finite-size extrapolation errors are smaller than the symbol size.

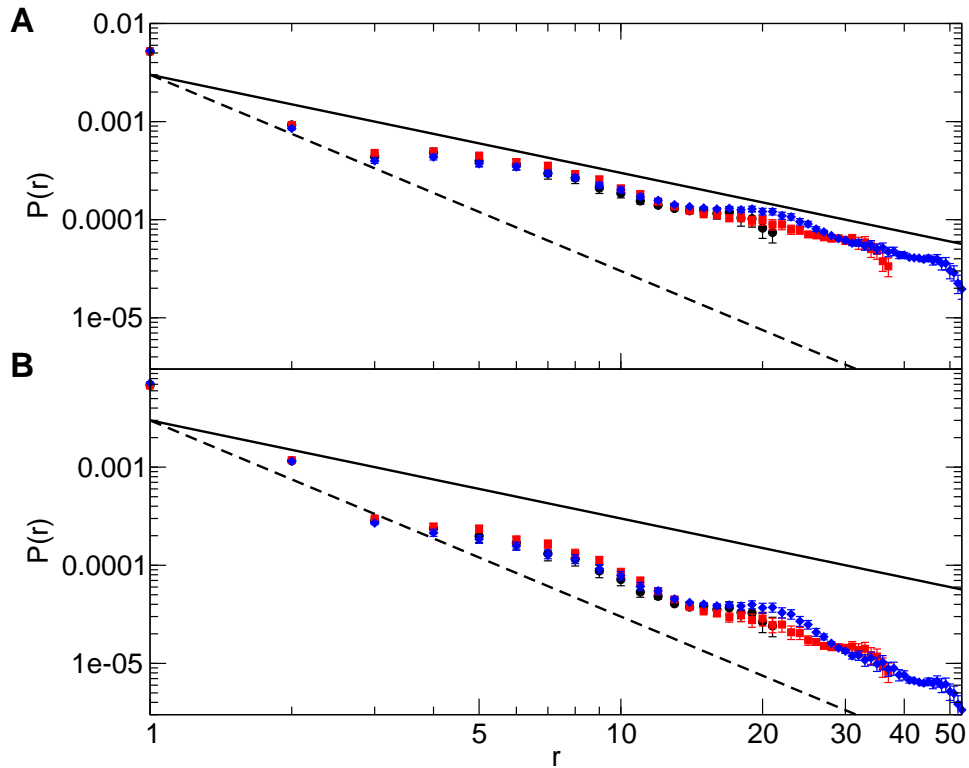


Figure 3: (Color online) Pair-pair correlation function $P(r)$ with $U_d = 8$ and doping $\delta = 0.0625$ as a function of the rung-rung distance r , for (a) $U_p = 0$ and $t_{pp} = 0$, and (b) $U_p = 3$ and $t_{pp} = 0.5$. Circles, squares, and diamonds are for 32, 48, and 64 rung ladders, respectively. $P(r)$ data is extrapolated in the DMRG truncation error; error bars are calculated from lattice averaging (see text). The solid (dashed) lines are power laws r^{-1} (r^{-2}).

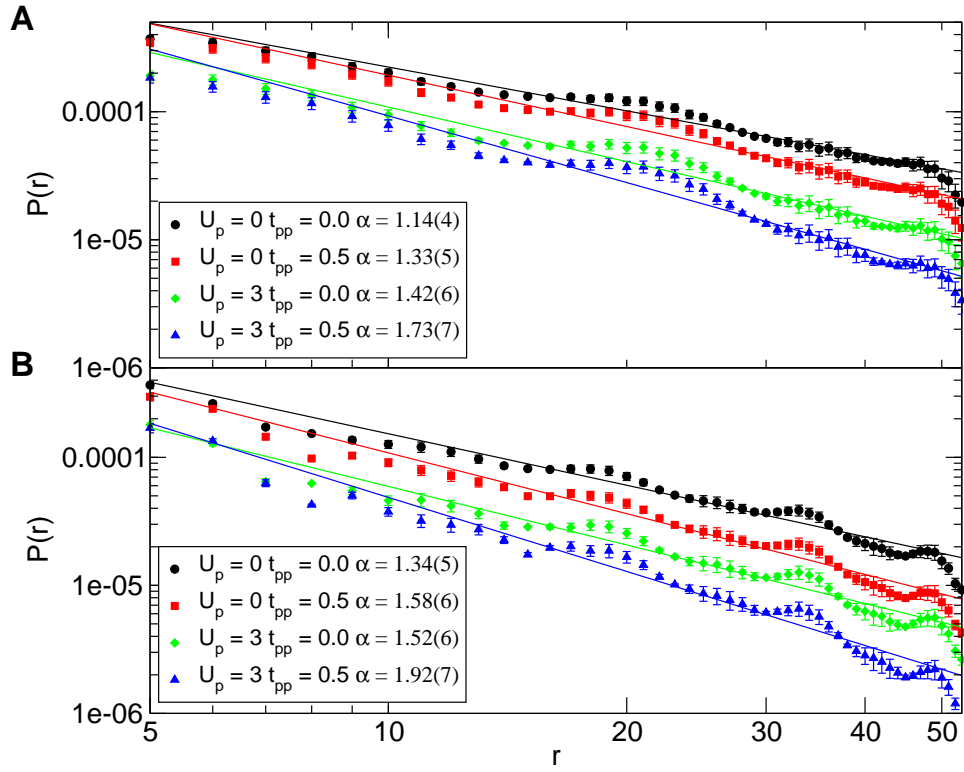


Figure 4: (Color online) $P(r)$ as a function of the rung-rung distance r for a 64-rung ladder with $U_d = 8$, for (a) doping $\delta = 0.0625$, and (b) $\delta = 0.1250$. Lines are linear fits of $P(r)$ for $10 \leq r \leq 45$; the power law exponents α are given in the figure legends.